

2017

Real-time Interactive Tractography Analysis for Multimodal Brain Visualization Tool: MultiXplore

Saeed M. Bakhshmand
Western University, smandiza@uwo.ca

Sandrine de Ribaupierre
Western University

Roy Eagleson
Western University

Follow this and additional works at: <https://ir.lib.uwo.ca/anatomypub>

 Part of the [Anatomy Commons](#), and the [Cell and Developmental Biology Commons](#)

Citation of this paper:

Bakhshmand, Saeed M.; de Ribaupierre, Sandrine; and Eagleson, Roy, "Real-time Interactive Tractography Analysis for Multimodal Brain Visualization Tool: MultiXplore" (2017). *Anatomy and Cell Biology Publications*. 64.
<https://ir.lib.uwo.ca/anatomypub/64>

PROCEEDINGS OF SPIE

SPIDigitalLibrary.org/conference-proceedings-of-spie

Real-time interactive tractography analysis for multimodal brain visualization tool: MultiXplore

Saeed M. Bakhshmand
Sandrine de Ribaupierre
Roy Eagleson

Real-time Interactive Tractography Analysis for Multimodal Brain Visualization Tool: MultiXplore

Saeed M. Bakhshmand ^a, Sandrine de Ribaupierre ^b, and Roy Eagleson^c

^aBiomedical Engineering Graduate Program, Western University, London, ON, Canada

^bDepartment of Clinical Neurological Sciences, Western University, London, ON, Canada

^cDepartment of Electrical and Computer Engineering, Western University, London, ON, Canada

ABSTRACT

Most debilitating neurological disorders can have anatomical origins. Yet unlike other body organs, the anatomy alone cannot easily provide an understanding of brain functionality. In fact, addressing the challenge of linking structural and functional connectivity remains in the frontiers of neuroscience. Aggregating multimodal neuroimaging datasets may be critical for developing theories that span brain functionality, global neuroanatomy and internal microstructures. Functional magnetic resonance imaging (fMRI) and diffusion tensor imaging (DTI) are main such techniques that are employed to investigate the brain under normal and pathological conditions. fMRI records blood oxygenation level of the grey matter (GM), whereas DTI is able to reveal the underlying structure of the white matter (WM). Brain global activity is assumed to be an integration of GM functional hubs and WM neural pathways that serve to connect them. In this study we developed and evaluated a two-phase algorithm. This algorithm is employed in a 3D interactive connectivity visualization framework and helps to accelerate clustering of virtual neural pathways. In this paper, we will detail an algorithm that makes use of an index-based membership array formed for a whole brain tractography file and corresponding parcellated brain atlas. Next, we demonstrate efficiency of the algorithm by measuring required times for extracting a variety of fiber clusters, which are chosen in such a way to resemble all sizes probable output data files that algorithm will generate. The proposed algorithm facilitates real-time visual inspection of neuroimaging data to further the discovery in structure-function relationship of the brain networks.

Keywords: Diffusion Tensor Imaging, functional MRI, Multimodal, Interactive Visualization, Fiber Tractography, Collision Detection

1. INTRODUCTION

1.1 Multimodal neuroimage data visualization

Proper planning and guidance of central nervous system neurosurgical procedures has a major effect in reducing of associated risks such as postoperative neurological deficits, for example simple sensory motor function or more complex cognitive problems. Achieving brain eloquence preservation during neurosurgical interventions is contingent upon adequate knowledge of how the brain functions and demands a thorough investigation of underlying tissues in the planning stage by employing brain 3D images. Modelling brain anatomy and functionality as a complex network for both neurological disorders and normal conditions is becoming main stream research in discovering how brain executes cognitive and motor tasks. This type of network, often called a functional or structural connectivity, is formed based on measurements from functional (e.g. fMRI, Positron Emission Tomography,¹ Magnetoencephalography²) or structural (e.g. T1 weighted MRI,³ diffusion weighted imaging⁴ (DWI)) brain imaging modalities. One of the major milestones in connectivity research area is examining functional and structural relation as a promising method to unravel neural basis of brain activity. Undoubtedly, fMRI and DTI are two important in vivo imaging modalities to quantify respective interactions. DTI data is the basis for generating virtual 3D model of actual axonal linkages in the brain called fiber tracts that serve to non-invasively identify configuration of WM bundles around intervention site and access trajectory.

Send correspondence to Saeed M. Bakhshmand Email: smahdiza@uwo.ca

Due to this fact, aggregation of multimodal neuroimaging data has been very popular among neuroscientists.⁵ Visualization has a crucial role in assisting a researcher to picture mutual information of dual modalities. It should be noted, that due to large quantity of processed information for each volume, exploration is a key component to enable user to view desired content in the anatomical space, selectively. This was a key consideration in designing and development of MultiXplore.⁶ In addition, this platform can visually integrate functional landmarks from an atlas parcellated brain and mutually intersecting fiber tracts. This unique visualization technique allows user to interactively inspect underlying WM pathways of functionally connected areas and aims to improve current knowledge of anatomical foundation serving brain networks. One of the main requirements of this visualization framework was minimization of system response time to achieve real time user interactions. This paper introduces a new technique to minimize computation time of fiber analysis algorithms.

1.2 Related works

Whole brain fiber tracts are densely populated inside of the brain, making it cumbersome to comprehend abnormalities within that limited space.⁷ Fiber clustering techniques have been used to group and classify fiber bundles of the WM to visualize them as subsets of whole brain tractography. Criteria for this classification is variant from shape similarity of adjacent fibers⁸ and originating/crossing from a given region of the brain⁹ to fMRI based inferential of fiber clusters.¹⁰ Chamberland et. al.¹¹ considered user interaction feature in a 3D environment to visualize fiber tracts originating from an interactive seed volume. Their algorithm employs an accelerated fiber tracking technique that supports real time generation of fiber tracts in the case of seed region displacement or parameter adjustment.¹² Weiler et. al.¹³ introduced a tool to assist with defining anatomically meaningful region(s) of interest (ROI) for fiber tract extraction. A tree-based data structure was utilized to store fiber information for interaction stage. A similar strategy was considered to facilitate fiber extraction from a whole-brain tractography. Optimizing required time to render the selected fibers is the main requirement for exploration of the large fiber bundles. The original contribution of this work extends upon a fiber selection algorithm used in fiber bundle label select (FBLs)¹⁴ to optimize its run time. This happened by generating a membership array to facilitate interactive visualization and selection of tracts in a real-time fashion. The module is developed within the framework of the 3D Slicer software platform.¹⁵

In this paper, a summary of imaging inputs for the algorithm is provided and data structure of the outputs is defined. In the results sections, we will represent generated fiber bundles and will compare required time of the new method to the current tools.

2. COMPUTATIONAL MODEL FOR FIBER CLUSTERING AND RETRIEVAL

2.1 DWI, DTI and Brain fiber tractography

DWI is a non-invasive medical imaging modality that relies on diffusion of water molecules inside of a tissue to generate structural images that indicates macrostructure of that tissue¹⁶(Figure 1a). DTI is the outcome of a mathematical operation on DWI images and computes distribution of major orientation of gradient directions in each voxel of the target tissue (Figure 1b). Parameters that are derived from tensors in DTI can be visualized as scalar values over brain volume. Other application of tensors are generating neural pathways by tracing voxel-level major orientation vectors. This process is called tractography (Figure 1f) and two major types are probabilistic and deterministic.¹⁷ Probabilistic method considers all possible tree branches of a neural fiber in a voxel with nonsignificant difference between first and second eigenvector, thus results in multiple tracks from a single seed region. Deterministic method prioritizes only one path for the fiber, without considering relative eigenvectors and generates a view of brain WM pathways that is more realistic and resembles actual brain WM anatomy.

2.2 Brain landmarks and parcellation

Brain atlas is a segmentation of brain volume to isolated subsets of regions that share similar anatomical, physical or functional properties. It provides a universal platform to label the brain regions across a large population of subjects. These labels can later be registered to the T1 weighted image and represent areas that share similar features. More details are shown in figure 2b and 2c.

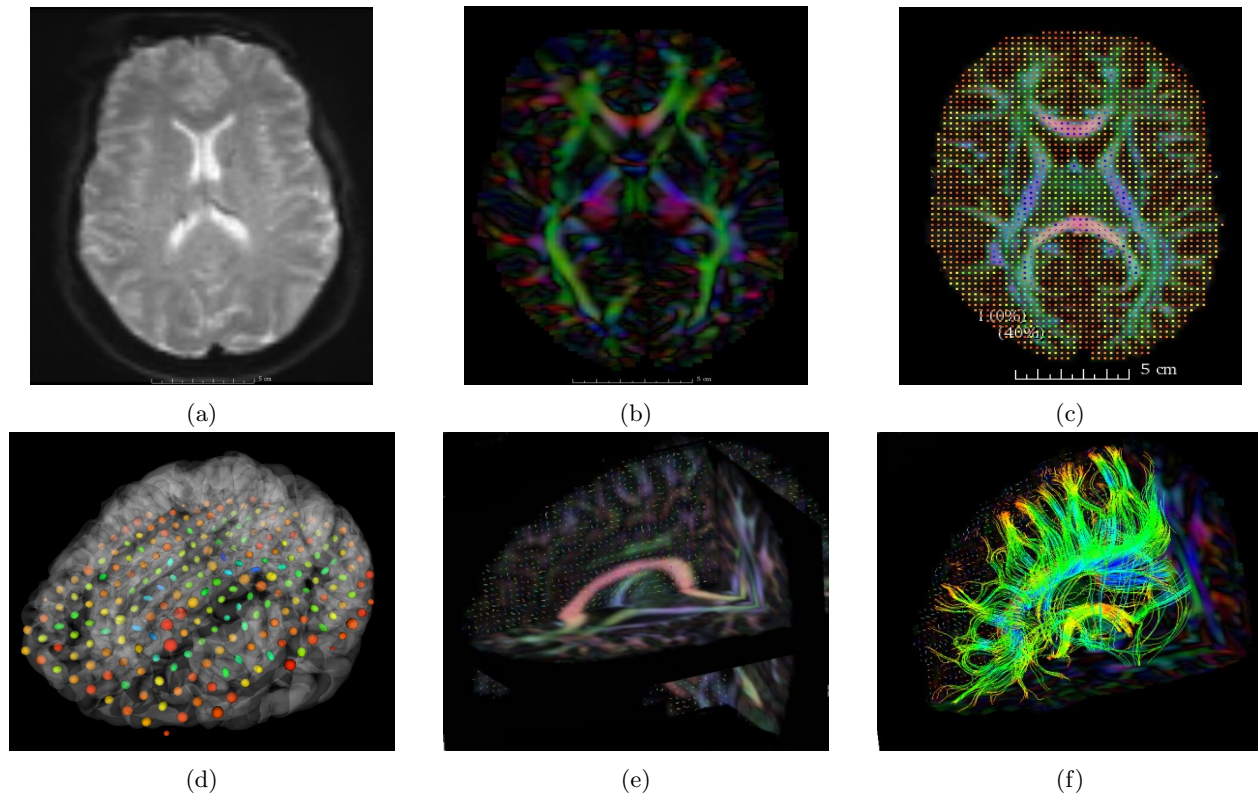


Figure 1: Basics of DTI and tractography: a) Eddy corrected DWI image b) DTI image constructed by painting voxels based on 3D orientation of their major diffusion gradient. Major diffusion orientation may be visualized as a 3D ellipsoid and overlaid on 2D slices (c) or 3D volumes (d) in a selected slice of the volume. d) uses line segments instead of ellipsoid to visualize voxel level diffusion tensors. As shown in (f) Voxel by voxel tracing for the major orientation of diffusion tensors constructs fibers that cross through that plane.

2.3 Functional connectivity

Functional MRI is a non-invasive MRI modality that records brain activity based on measuring consumed energy of that activity: oxygen. In other words, fMRI can spatially differentiate areas that demand higher oxygenated blood supply with an acceptable temporal resolution. Basic assumption of fMRI is originated from the fact that higher brain activity necessitates more oxygenated blood at a given area. These activation signals are recorded along the time while subject of the study is in the MRI scanner performing designed tasks. As a result, fMRI yields a temporal signal of BOLD response in each brain region within the determined field of view. Functional connectivity is a computational approach to analyze fMRI signal all over the brain and aims to find recurrent patterns of brain activity between different regions of the brain and along the recorded window of experiments. Connectivity can be modelled as graph with nodes located in atlas areas of the brain and strength of between-node similarity is represented as graph edges. Similar to graph theory, a matrix can hold and represent numerical values of graph connections in a compact fashion. Atlas defined subvolumes (here we call them ROI) of the brain serve as nodes of the connectivity graph. Functional MRI signals of the corresponding nodes are obtained from these subvolumes of the GM.

2.4 VTK Fiber Bundle data structure

Here we will review data structure of a VTK¹⁸ file that is employed to display and store results of fiber tractography in 3D Slicer. As shown in figure 3a, a deterministic fiber tractography file consists of a finite number of lines. Each line has an identifier index that uniquely represents that particular line. Second level is the number of spatial points that exist inside of any given line. Those set of point coordinates are an attribute of the line. Another attribute of the line is principal diffusion gradients of any corresponding voxel along the line that is

saved in a 3×3 tensor unit holds three eigenvectors of each point and is used to render colors of the fibers according to the parameters of choice for the user.

2.5 Atlas registered brain

Outcomes of the brain atlas parcellation are saved in a 3D volume with same coordinate system as original file. Main difference between a normal volumetric structural brain scan (Figure 1b) and atlas volume (Figure 1c) is narrowed to voxel values. Volume content of the atlas, instead of grey level values, are integers that represent labels of the region every given voxel is associated during registration. This label file serves to determine which atlas region any given point of a fiber belongs to (figures 2e and 2d).

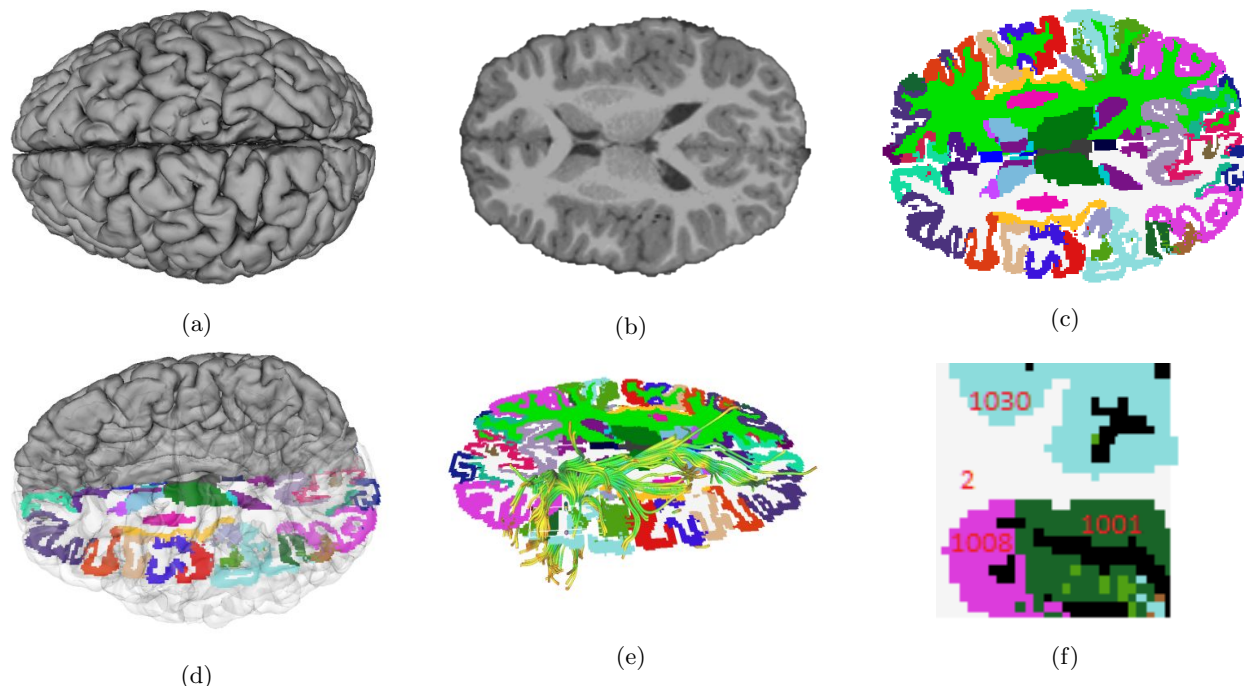


Figure 2: Brain Atlas Parcellation: a) Cortical 3D surface generated by FreeSurfer¹⁹ b) One axial slice of a T1 weighted volume c) One axial slice of resulted atlas registration: This a DK Atlas that is registered to subject space using FreeSurfer. Each color represents voxels that belong to the same label. d) Corresponding location of the slice compared to brain volume. Left hemisphere cortical mesh is translucent to allow see the labels. e) Subset of fibers that pass through a selected rectangular area over the chosen slice. f) Magnified view of the rectangular area in (e) with numeric equivalent of the labels manually added to the image.

2.6 Coordinate system transformation

Since tractography lines and atlas registered labeled brain volumes might depend on different coordinate systems, it is wise to inspect whether a transformation for projecting labeled file to tractography file space is required or not. For instance, in our data, tractography was performed in scanner space (IJK) coordinate system, while label file was in subject space (RAS) and was transformed to IJK space during the memory array generation process.

2.7 Memory array, Label lookup table (LUT) and memory points

Our proposed algorithm imports a set of spatial maps accessed via a parcellated brain atlas. These maps can later be used to verify whether a line enters into that region or not. The main task of the proposed algorithm is to iterate through each point of every given line and distinguish which spatial map each point under investigation belongs to, and record it in a membership array. As figure 3b illustrates, concatenation of these 1D

binary vectors forms the final 2D array that will be stored and referred during interaction stage. The number of rows is equal to the number of brain atlas regions that intersect fibers and the number of columns is same as number of lines in the main tractography file. There are two other data segments that are generated during memory array processing: memory points and label lookup table. Memory points obtains number of points in each individual line and stores them as a 1D array with a length equal to the number of lines in tractography file. Similarly, label look up table (LUT) is the other 1D array that stores integer value of the engaged labels in the same order of memory array with a size equal to the number of engaged labels. Upon the users selection, the selected rows of the memory array will be element-wise multiplied, producing a vector with the same size (Figure 4). This new array contains indices of the lines that are added to the scene in every iterative selection.

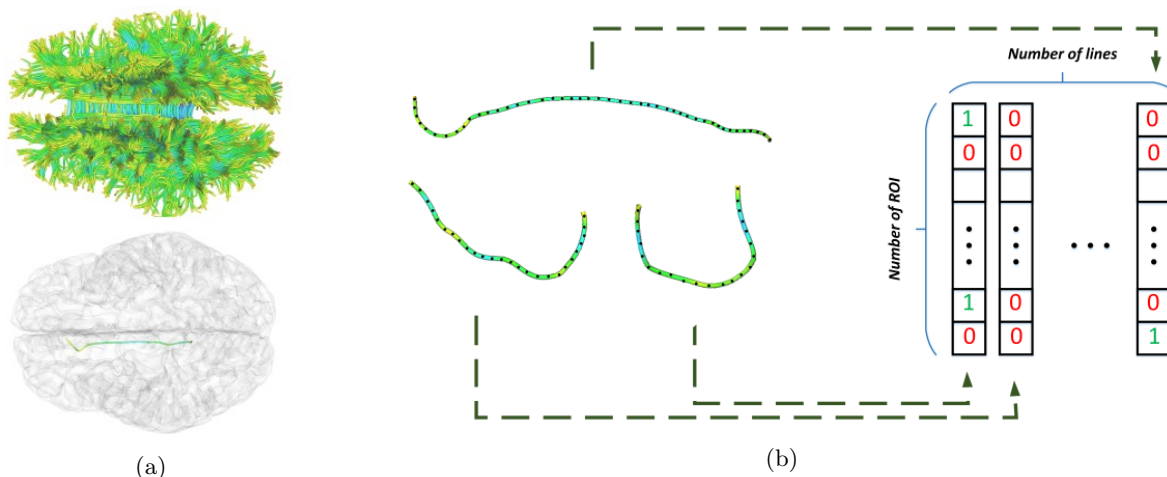


Figure 3: Formation of membership array: a) Whole brain fiber tractography and A single streamline b) Scanning of streamlines according to brain labels to generate membership array.

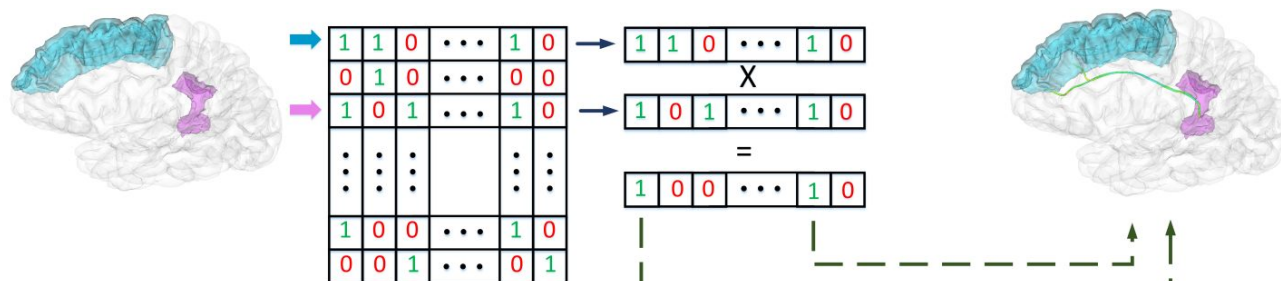


Figure 4: Processing of users input from a user interface developed in MultiXplore,⁶ from left to right: rows of selected ROIs are multiplied and corresponding streamlines are transferred into 3D view.

3. RESULTS

In order to test efficiency of the proposed algorithm, three sets of experiments are carried out. First one examines processing times required to generate memory arrays for whole-brain tractography files with a variety of line densities. Next two experiments allow us to compare outcomes of our method to two other available tools with similar functionality: FBLS and tractography label map seeding (TLMS).¹⁴

Second one aims to investigate required time to transfer selected tracts upon user's selection. In this test, acquired times from our method are compared to FBLS. Similar to the second one, third experiment reports the required time for extracting a subset of fibers. Main difference from second experiment is being restricted to one ROI at very repetition. Our proposed algorithm (Pre-computed Array) and FBLS have the potential to accept multiple regions as input. TLMS is the other module in 3D Slicer that can generate ROI based fiber bundles.

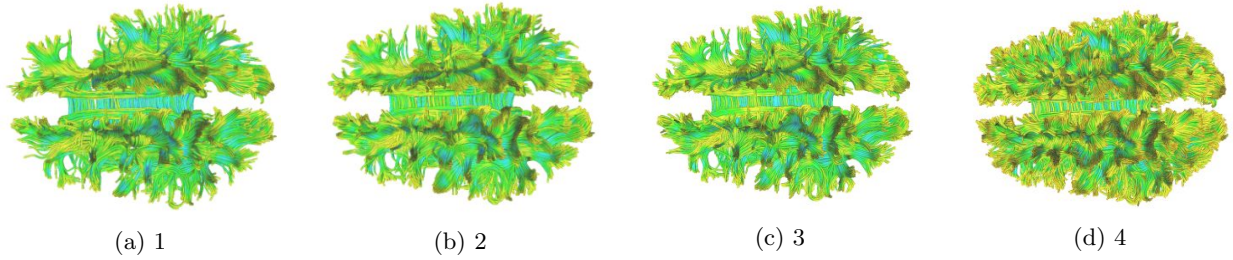


Figure 5: Axial views of tractography files with low (a) to high (d) line densities

TLMS performs the fiber subset generation differently than FBLs. It performs tractography by seed placement inside of the designated volume. Sole limitation of this module is being restricted to one ROI at a time. Due to tractography procedure, where fibers can't be filtered to retain the ones that pass through multiple ROIs. Anatomical scan and DTI data used in this study are from a 30 year old healthy subject. Cortical surface and registration of desikan-killiany Atlas labels is done using FreeSurfer (<http://surfer.nmr.mgh.harvard.edu/>).

These tests have been carried out in the imaging platform of 3D Slicer version 4.5.0-1 using a Windows 10 PC (24 GB DDR3 RAM, Intel core i7 CPU 64 bit). FBLs and TLMS are loadable modules in 3D Slicer, built as C++ plugins and optimized for heavy computations. Pre-computed array is written in Python and implemented as a scripted module to prototype the novel idea. Inputs for preprocessing algorithm are 4 tractography files prepared by 3D Slicer from DTI images and with varying seed spacing parameter to prepare a range of line numbers and observe its effect on the computation time. Other tractography parameters are identical for all four scenarios and are as follow: linear measure start threshold: 0.3, minimum path length: 10mm, maximum path length: 800mm, stopping criteria: fractional anisotropy (FA), stopping value: 0.2, Stopping Track Curvature: 0.6, Integration Step: 0.5mm. Table 1 outlines number of lines and points in the generated fibers, as well as spacing of the seed in tractography stage and required time to generate precomputed memory array, memory points and LUT. Figure 5a to 5d exhibits generated data. By visual inspections of those 4 data we decided to set seed spacing to 0.5 mm for input file of the next step. Fibers in all the figures are colored according to the voxel level FA and a rainbow colormap.

Table 1: Properties of generated tractography files and required preprocessing times in seconds

	Number of Lines	Number of Points	Seed Spacing(mm)	Computing time(s)
1	3527	296977	3	4
2	1696	989244	2	9
3	54559	4593416	1.2	34
4	172553	14169565	0.5	106

Table 2: Considered single ROI for evaluating required wait time: lh and rh refers to left hemisphere and right hemisphere respectively, reported times are in seconds.

Index of ROI	Selected Region Atlas Label	Num. of Points	Num. of Lines	TLMS (s)	Num. of Points	Num. of Lines	FBLs (s)	Memory Array (s)
1	Temporalepole(rh)	80751	1154	11	92755	1204	62	6
2	Superiortemporal(lh)	252892	3823	14	275340	3180	64	20
3	Superiorfrontal(rh)	1074906	14599	28	940236	11059	67	150

In the next experiment, fiber bundle selection base is single ROI. According to table 2 and figure 6 three regions are considered. Generated fibers from TLMS had slightly different characteristics than FBLs and our method, therefore we reported their number of points and lines in a separate column. For the third experiment, we found 5 combinations of ROIs that enabled testing FBLs and our method on a fiber bundle with minimum

of 18 and maximum of 3420 lines. Figure 7 shows spatial configuration of the processed fiber bundles. Likewise, table 3 reports the numerical outcomes of this experiment.

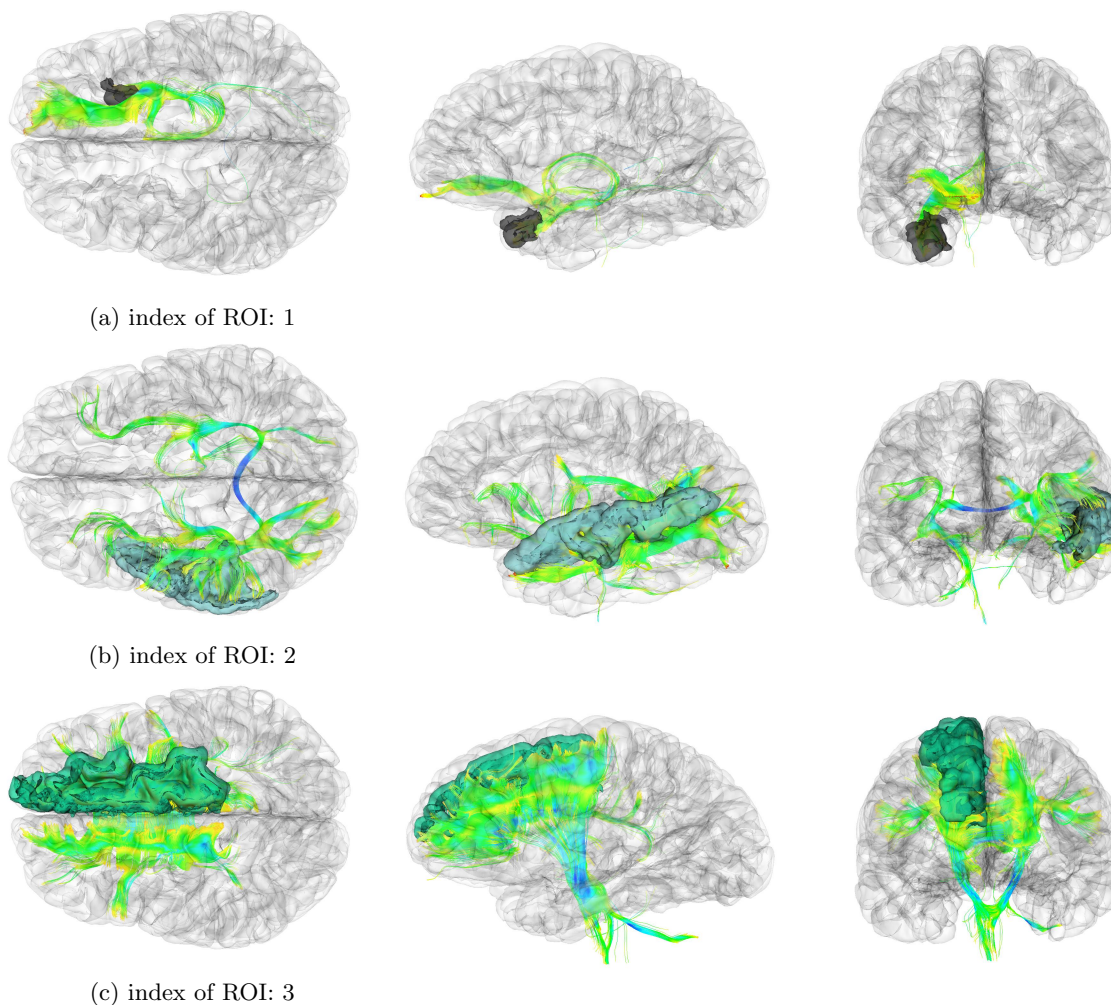


Figure 6: Axial, Sagittal and Coronal views of the extracted tracts with highlighted atlas labels in color along with a cortical surface to ease anatomical localization, numbers in the left indicate Index of selected ROI from Table 2

4. DISCUSSION

The proposed algorithm demonstrates an improved speed on ROI-based fiber bundle extraction, compared to FBLS. In the first experiment and according to table 1 we observed that line and point density of the fiber tractography is the main factor to determine the necessary time for memory arrays computation. As can be seen from time performance of table 6, TLMS holds a significantly better time performance than other two methods. For instance, Superiorfrontal region takes 28 seconds for TLMS compared to 150 seconds of precomputed array. However and as stated above, main limitation of TLMS is being confined to one ROI, therefore fiber pathways between separate ROIs cannot be found.

According to the table 3 (last column) required time for memory array method is proportional to the fiber bundle density. On the other hand, FBLS operation is divided into two steps. No matter how large or small the output fibers would be, first step takes around 60 seconds for each selection to scan the fiber bundle and create a temporary memory array and second step takes 2 to 8 seconds for considered ROIs and is intended

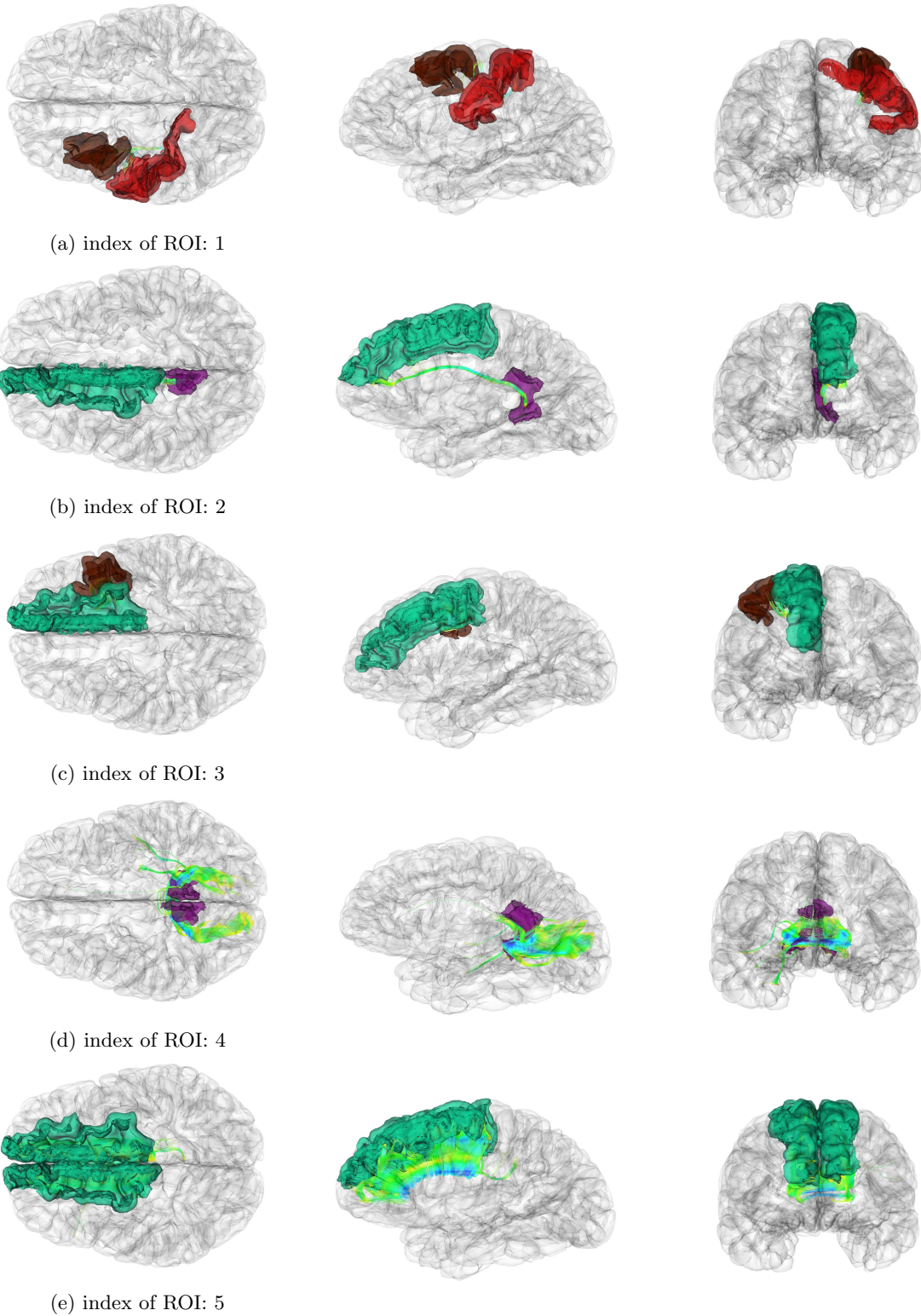


Figure 7: Axial, Sagittal and Coronal views of some of the extracted tracts with highlighted atlas labels in color along with a cortical surface to ease anatomical localization, numbers in the caption indicate Index of selected ROI from Table 2

Table 3: Considered pairs of ROIs for evaluating required wait time: lh and rh refers to left hemisphere and right hemisphere respectively, reported times are in seconds.

Index of ROI	Selected Region(s) Atlas Label	Num. of Points	Num. of Lines	FBLs (s)	Memory Array (s)
1	CaudalMiddleFrontal(lh) and PostCentral(lh)	1843	18	62	≤ 1
2	SuperiorFrontal(lh) and IsthmusCingulate(lh)	9916	88	64	1
3	SuperiorFrontal(rh) and CaudalMiddleFrontal(rh)	7029	175	64	3
4	IsthmusCingulate(lh) and IsthmusCingulate(rh)	93233	923	65	9
5	SuperiorFrontal(lh) and SuperiorFrontal(rh)	311155	3420	68	32

for copying selected fibers. Despite lengthier total required time in FBLs, copying fibers happens in much faster speed compared to memory array. This is due to the inherent speed differences of C++ compared to Python. It should be noted that our current implementation is a scripted module (based on Python); whereas FBLs or TLMS modules C++ plugin (called loadable module) built against 3D Slicer and have access to more efficient processing power. Despite this, overall computation time for largest dual ROI selection (left and right Superiorfrontal, last row of table 7) in precomputed array achieves 32 seconds, less than half of the similar time for FBLs (67 seconds).

5. CONCLUSION

In this paper a novel fiber selection algorithm is presented This algorithm improves run time of FBLs by optimizing redundant operations. This improvement leads to adapt the new method in a multimodal visualization framework of fMRI and DTI that intends to visualize the anatomical origins of brain functional hubs during neurosurgical treatments, as well as clinical research, and for neuroscientific enquiry.

In this paper, we presented a novel algorithm that significantly reduces required time for fiber clustering. This has been realized by dividing a fiber selection pipeline to two stages and performing first stage that results in a membership array which helps to reduce the required time for the second stage. This method contributes to relatively low wait time and an ultimate key role in implementation of MultiXplore.⁶ Time requirement for the first stage depends on the volume of the input tractography file and varies from 1 to 3 minutes for an adequately dense tractography data in the current system. According to our tests and results, the required time for the second stage is dependent on the number of lines and never exceeds 1 minute for the largest probable selection. This is due to the fact that copying lines takes place in an iterative loop. FBLs wasn't designed to support timely responses to user's multiple queries and consequently user might end up waiting for several minutes. Therefore, a new approach was needed to minimize the time and allow for smooth exploration of multimodal brain imaging data. Such an exploration would be beneficial in visualization of brain structural-functional relations. In future we plan to transfer our implementation to C++ to further acceleration of the fiber extraction process.

ACKNOWLEDGMENTS

We would like to thank Dr. Ali Khan for his help with DWI data analysis and Dr. Lauren O'Donnell and 3D Slicer community for helping with fiber extraction process. Funding for this project was provided by Grande-NCE and National Science and Engineering Council of Canada (NSERC).

REFERENCES

- [1] Frackowiak, R. S., Lenzi, G.-L., Jones, T., and Heather, J. D., “Quantitative measurement of regional cerebral blood flow and oxygen metabolism in man using ^{15}O and positron emission tomography: theory, procedure, and normal values.,” *Journal of computer assisted tomography* **4**(6), 727–736 (1980).
- [2] Hämäläinen, M., Hari, R., Ilmoniemi, R. J., Knuutila, J., and Lounasmaa, O. V., “Magnetoencephalography theory, instrumentation, and applications to noninvasive studies of the working human brain,” *Reviews of modern Physics* **65**(2), 413 (1993).
- [3] Mansfield, P., “Multi-planar image formation using nmr spin echoes,” *Journal of Physics C: Solid State Physics* **10**(3), L55 (1977).
- [4] Moseley, M. E., Cohen, Y., Kucharczyk, J., Mintorovitch, J., Asgari, H., Wendland, M., Tsuruda, J., and Norman, D., “Diffusion-weighted mr imaging of anisotropic water diffusion in cat central nervous system.,” *Radiology* **176**(2), 439–445 (1990).
- [5] Zhu, D., Zhang, T., Jiang, X., Hu, X., Chen, H., Yang, N., Lv, J., Han, J., Guo, L., and Liu, T., “Fusing dti and fmri data: a survey of methods and applications,” *NeuroImage* **102**, 184–191 (2014).
- [6] Bakhshmand, S. M., de Ribaupierre, S., and Eagleson, R., “Multixplore: Multimodal exploration platform for collocated functional and structural connectivity,” in [*Organization for Human Brain Mapping annual meeting*], (2016).
- [7] Eichelbaum, S., Wiebel, A., Hlawitschka, M., Anwander, A., Knösche, T. R., and Scheuermann, G., “Visualization of effective connectivity of the brain.,” in [*VMV*], 155–162 (2010).
- [8] Ge, B., Guo, L., Zhang, T., Hu, X., Han, J., and Liu, T., “Resting state fmri-guided fiber clustering: methods and applications,” *Neuroinformatics* **11**(1), 119–133 (2013).
- [9] Wang, Q., Yap, P.-T., Wu, G., and Shen, D., “Application of neuroanatomical features to tractography clustering,” *Human brain mapping* **34**(9), 2089–2102 (2013).
- [10] Li, X., Lim, C., Li, K., Guo, L., and Liu, T., “Detecting brain state changes via fiber-centered functional connectivity analysis,” *Neuroinformatics* **11**(2), 193–210 (2013).
- [11] Chamberland, M., Bernier, M., Fortin, D., Whittingstall, K., and Descoteaux, M., “3D interactive tractography-informed resting-state fMRI connectivity,” *Frontiers in Neuroscience* **9**(August), 1–15 (2015).
- [12] Chamberland, M., Whittingstall, K., Fortin, D., Mathieu, D., and Descoteaux, M., “Real-time multi-peak tractography for instantaneous connectivity display,” *Frontiers in neuroinformatics* **8**(May), 59 (2014).
- [13] Weiler, F. and Hahn, H. K., “An interactive ROI tool for DTI fiber tracking,” *Imaging* **7964**, 796437–796437–7 (2011).
- [14] Farhat, N., Kapur, T., Kikinis, R., “Role of Computers and Image Processing in Image-Guided Brain Tumor Surgery,” in [*Image-Guided Neurosurgery*], (2015).
- [15] Pieper, S., Halle, M., and Kikinis, R., “3D Slicer,” *2004 2nd IEEE International Symposium on Biomedical Imaging: Nano to Macro (IEEE Cat No. 04EX821)* **2**, 632–635 (2004).
- [16] Le Bihan, D., Breton, E., Lallemand, D., Grenier, P., Cabanis, E., and Laval-Jeantet, M., “Mr imaging of intravoxel incoherent motions: application to diffusion and perfusion in neurologic disorders.,” *Radiology* **161**(2), 401–407 (1986).
- [17] Mori, S. and van Zijl, P., “Fiber tracking: principles and strategies—a technical review,” *NMR in Biomedicine* **15**(7-8), 468–480 (2002).
- [18] Schroeder, W. J., Martin, K. M., and Lorensen, W. E., “The design and implementation of an object-oriented toolkit for 3d graphics and visualization,” in [*Proceedings of the 7th conference on Visualization'96*], 93–ff, IEEE Computer Society Press (1996).
- [19] Reuter, M., Schmansky, N. J., Rosas, H. D., and Fischl, B., “Within-subject template estimation for unbiased longitudinal image analysis,” *Neuroimage* **61**(4), 1402–1418 (2012).